Advances in Research

20(4): 1-25, 2019; Article no.AIR.53521
ISSN: 2348-0394, NLM ID: 101666096

Numerical Investigation on Steel Square HSS Columns Strengthened with Polymer-mortar

Khaled M. El-Sayed[1], Ahmed S. Debaiky[1], Nader N. Khalil[1] and Ibrahim M. El-Shenawy[1*]

[1]Department of Civil Engineering, Benha Faculty of Engineering, Benha University, Benha, Egypt.

Authors' contributions

This work was carried out in collaboration among all authors. All authors read and approved the final manuscript.

Article Information

DOI: 10.9734/AIR/2019/v20i430164
Editor(s):
(1) Dr. Martin Kröger, Professor, Computational Polymer Physics, Swiss Federal Institute of Technology (ETH Zürich), Switzerland.
Reviewers:
(1) Shashidhar K. Kudari, CVR College of Engineering, India.
(2) Bou Azza, University of Bechar, Algeria.
Complete Peer review History: http://www.sdiarticle4.com/review-history/53521

Original Research Article

Received 13 October 2019
Accepted 23 December 2019
Published 28 December 2019

ABSTRACT

This paper presents the results of finite element (FE) analysis of axially loaded square hollow structural steel (HSS) columns, strengthened with polymer-mortar materials. Three-dimensional nonlinear FE model of HSS slender columns were developed using thin-shell element, considering geometric and material nonlinearity. The polymer-mortar strengthening layer was incorporated using additional layers of the shell element. The FE model has been performed and then verified against experimental results obtained by the authors [1]. Good agreement was observed between FE analysis and experimental results. The model was then used in an extended parametric study to examine selected AISC square HSS columns with different cross-sectional geometries, slenderness ratios, thicknesses of mortar strengthening layer, overall geometric imperfections, and level of residual stresses. The effectiveness of polymer-mortar in increasing the column's axial strength is observed. The study also demonstrated that polymer-mortar strengthening materials is more effective for higher slenderness ratios. An equivalent steel thickness is also accounted for the mortar strengthened HSS columns to discuss the effectiveness of polymer-mortar strengthening system. The polymer-mortar strengthening system is more effective for HSS columns with higher levels of out-of-straightness. Level of residual stress has a slight effect on the gain in the column's axial strength strengthened with polymer-mortar.

**Corresponding author: E-mail: ibrahim.alshenawi@bhit.bu.edu.eg;*

Keywords: Finite element; buckling; HSS; column; polymer; mortar.

1. INTRODUCTION

In recent years, the use of high yield steel and slender cross-sections has become an economical solution in steel construction for low-rise buildings. The cold-formed sections have some characteristics although combination of section's high yield strength and element slenderness that leads to local instability with reduced section capacity in compression and bending. Columns are generally the most important element in a structure that need to be strengthened. The most critical load that controls the stability of thin shells is the axial compression, Torabi and Shariati [2]. Under compression, component plates comprising the cold-formed steel member commonly buckle before overall failure. Stiffness of the member against overall bending or torsion is fundamentally affected by the local buckling. This can cause the early failure of the column, and reduces the load capacity of the member, Jaehong et al. [3]. The capacity of cold-formed steel columns mainly depends on its components local behavior and the overall behavior of the column.

There are certain buckling modes exist in open steel cold-formed section (such as C, Z, and hat section) due to their mono-symmetry, shear center eccentricity centroids, high plate slenderness, and low torsional rigidity. Thus, hollow structural section (HSS) steel columns have recently become popular in the steel construction industry, Bambach [4], Law and Gardner [5]. They are produced in different cross-section geometries such as compact, non-compact and slender sections according to the appropriate international steel specification. Key and Hancock [6] investigated the column behavior of square hollow steel cold-formed sections with slenderness ratio ranging from 66 to 98. Vieira et al. [7] presented a large parametric study on evaluating the critical local buckling coefficient for rectangular steel hollow cold-formed section (RHS) members subjected to combined axial load and biaxial bending.

Aged, damaged and overburdened steel structures need retrofitting to comply with the modified and more stringent recent design specifications. Strengthening of existing steel structural members is also be required to increase the structure capability to resist higher applied live loads. The use of Fiber Reinforced Polymer (FRP) materials is gaining popularity over conventional methods using steel plating for repairing and strengthening of steel structures, Zhao and Zhang [8]. Haedir and Zhao [9] experimented the behavior of externally bonded carbon fiber reinforced polymer (CFRP) sheets strengthened ten short steel circular hollow cold-formed section (CHS) columns. The results showed that CFRP strengthening the steel tube can enhance the axial capacity of the section. A wide range of thin-walled square hollow steel section geometries strengthened with carbon fibers bonded to the external surfaces of the steel tube walls were experimented by Bambach [4]. Shaat and Fam [10] presented an experimental investigation on steel square HSS slender columns having constant slenderness ratio. The columns was strengthened with high modulus HM-CFRP sheets. The results showed an increase in the column's axial strength up to 23%.

Such experimental investigations provide useful results regarding strengthening, however more data is still needed in this field. The major disadvantages of experimental tests over FE analysis are the time constraint and high cost of laboratory testing, thus hindering progress in composite research areas. A reliable FE analysis is often considered as an alternative to costly experimental procedures. There are numerous investigations carried out by various researchers in this area. Shaat and Fam [11] proposed an analytical model of his experimental study. The model predicted the load-axial and lateral displacements. The model also accounted for steel plasticity, out-of-straightness imperfections, residual stresses, geometric nonlinearity, and the CFRP contribution. Another study using non-linear FE analysis was completed and verified against both experimental and other analytical models, Shaat and Fam [12]. The FE model predicted ultimate loads and failure modes. The FE numerical analysis revealed that CFRP strengthening technique is generally more effective for HSS columns with higher slenderness ratios and larger geometric imperfections. Then, the study included high modulus HM-CFRP of 313 GPa and concluded that the effectiveness of CFRP strengthening long columns increases as slenderness ratio increases, Shaat and Fam [13]. The increase percentage in axial strength and stiffness ranged from 6 to 71% and 10 to 17%, respectively. Urmi

and Khan [14] investigated numerically using shell elements CFRP strengthening of square HSS columns (mild steel). Then, A parametric study was focused on selected non-compact AISC (American Institute of Steel Construction) steel square HSS columns. The study discussed the effects of number of CFRP strengthening layers, column slenderness ratio and cross-section geometry on the axial load capacity of columns. The study concluded that variation in strength is less significant in columns with short and intermediate lengths. Ritchie et al. [15] investigated the behavior of steel long columns having slenderness ratio of 197 strengthened using CFRP plates of various moduli. The increase percentage in axial strength ranged from 11 to 29%. The gain increased as initial out-of-straightness, CFRP modulus, or CFRP strengthening ratio increased. Despite their characteristics, FRP have some disadvantages such as; high costs, sensitivity to mechanical damage and fire resistance, lower ductility, poor shear strength, and low strain at failure.

The use of polymer-mortar has recently increased as replacement of regular mortar due to their advantages such as; high bond strength, high abrasion resistance, high freeze-thaw and fire resistance, increased bending, compressive and tensile strengths, durability, and good chemical resistance in hard environments. Liu X. et al. [16] presented the results of experimental and analytical study on a retrofitting method of corroded steel columns. FRP jackets were wrapped around the corroded steel columns, and then filled with an expansive light-weight concrete. The strengthened specimens failed in overall buckling with a gain in load bearing capacity ranged from 58-233%. Increased capacity of the strengthened specimens was still much lower than the yield capacity of the full section. El-Tawil and Ekiz [17] presented a new technique for preventing buckling response of the steel bracing using mortar. The strengthening method involves mortar blocks attached around single and double angle braces with FRP sheets wrapped outside. After strengthening, the ultimate compressive loading was enhanced from 52% to 200%. Feng P. et al. [18] improved buckling resistance of compressive steel members using a strengthening approach. FRP tube is filled with mortar outside the steel members and wrapped with FRP fabrics at the tube ends. The strengthening effect was analyzed by comparison of both theoretical and test results. The failure mode of steel yielding at mid-height of the steel member due to global buckling was changed to local damage at the end of the steel member. The maximum load bearing capacity of strengthened members increased by 44-215%. El-Sayed et al. [1] investigated experimentally an innovative strengthening system to improve buckling resistance of steel square HHS short and long slender columns using polymer-mortar; applied directly to outer steel surface. The used polymer-mortar is a combination of epoxy resins and selected quartz aggregates, commercially known as (SIKADUR-41CF) manufactured by SIKA® branch in Swiss. Both axial strength and axial stiffness of HHS slender columns were increased. The maximum strength of mortar-strengthened HSS slender columns was increased by up to 77%. Axial, lateral deflection, and axial strain were also reduced. The effectiveness of polymer-mortar strengthening system increased in HHS columns with higher slenderness ratios and larger initial out-of straightness imperfections.

Although their eminent advantages, more research is still needed to build sufficient background on the application of polymer-mortar as a strengthening material for steel members. This paper presents a three dimensional nonlinear FE model using thin-shell element to investigate theoretically the behavior and strength of steel square HSS slender columns strengthened using polymer-mortar, considering both material and geometric nonlinearities. Verification of this FE model has been demonstrated with reference to the experiments of El-Sayed et al. [1]. The proposed model is then used in an extended parametric study to examine some selected AISC [19] square HSS slender columns of different cross-sectional geometries, slenderness ratios, thicknesses of mortar strengthening layer, overall geometric imperfections, and level of residual stresses. Also, the equivalent increasing in steel thickness computed for different HSS columns strengthened with polymer-mortar in the parametric study. The model was also used to examine the different potential failure modes of mortar strengthened square HSS columns.

2. FINITE ELEMENT MODELING

2.1 Model Description

A non-linear finite element model was developed using ANSYS® [20] software program to predict the responses of mortar-strengthened steel HSS columns. The model accounts for both material

and geometric nonlinearities. Since this study was concerned on thin-walled structural sections, a four node isoparametric thin-shell element (SHELL181) has been used for steel square HSS columns. The element configurations as well as its coordinate system are shown in Fig. 1(a). This element has six degrees of freedom at each node, three translations in the x, y, and z directions, and three rotations about x, y, and z axes. It also allows for both material and geometric nonlinearities. The multiple layers of this element were utilized to account for distribution of the through-thickness residual stresses through the HSS steel wall thickness. To perform the FE model in a generalized manner, a hollow steel square section is selected in a way to ease modeling procedures. For example, modeling of rounded corners of the square HSS section is treated as flat junction. Strengthening polymer-mortar materials have been modeled with an additional equivalent layer of similar shell element. Here, perfect full bond has been assumed between strengthening layers and steel. This assumption is quite reasonable in the model as no signs of debonding were observed experimentally, El-Sayed et al. [1]. Mesh density should be selected using the appropriate aspect ratio of the element. The final mesh density of the model used in this study was chosen after a mesh refining process has been conducted. The entire specimen was modeled in this study as shown in Fig. 1(b). Only one quarter of the column can be modeled, by taking advantage of the double symmetry of the specimen cross-section. However, modeling of the complete specimen gives a clearer impression of the behavior of the whole column. In this study, the FE simulation consisted of two stages. In the first stage, an eigenvalue elastic buckling analysis that is available in the ANSYS program was carried out on a perfectly straight specimens, including modeling of the entire cross-sections. In this stage, a linear elastic isotropic analysis of the control specimens, in which the stiffness of the structural member remained unchanged. As such, only the values of Young's modulus (Es = 200 GPa), and Poisson's ratio of steel (υ = 0.30) were defined. Otherwise, in the second stage, a non-linear FE analysis was performed on the slender columns modeled with out-of-straightness geometric imperfections to develop the predicted buckling shape established through the first stage of analysis. The second stage of the numerical simulation included a non-linear analysis, in which the stiffness of the structural member changes as it deforms. Also in this stage, the columns were externally loaded till failure to predict their full responses and ultimate capacity. The steel non-linearity was accounted for the FE modeling by specifying a bi-linear isotropic hardening plasticity model. A nominal bilinear stress-strain curve for used steel HSS1 and HSS2, which obtained from experimental stub-column tests by El-Sayed et al. [1] are adopted in Fig. 1(c). The tangent modulus for the steel stress-strain curve was assumed equal to 0.5 percent of its elastic modulus as suggested by Bruneau M. et al. [21]. The polymer-mortar materials were defined as linear and elastic isotropic materials, namely, the Young's modulus of 9 GPa, as provided by the supplier for (Sikadur® -41CF). The hardening effect due to cold-rolling process was ignored. The average membrane residual stress is applied in the FE model as a pre-stress, which is kept constant while the externally applied load increases up gradually to the failure load. In order to model the hinged end condition of the columns, a thick, elastic and stiff steel plates were modeled at both ends of the column using the same shell element with controlled degrees of freedom. The rigid plates were also provided to ensure accurate stress distribution over the column section. Longitudinal dimension has been considered along the y-direction whereas cross sectional dimensions have been considered along x- and z-directions. The boundary conditions were selected to satisfy the pinned end conditions in accordance with the column's test, El-Sayed et al. [1]. At the loaded end, the translations in the transverse direction (Ux, and Uz) along the middle line of the rigid plate were restrained, whereas the translations in the longitudinal direction (Uy) along the same line were released. On the other hand, the translations in all the x, y and z direction at the unloaded end was prevented. The rotational degrees of freedom in all directions (Rx, Ry, and Rz) were released. Axial compressive loading was applied at the upper end as point loads on the perimeter of the specimen cross-section as in the experimental test setup. Non-linear analysis is performed by considering Newton-Raphson method. Fig.1 (b) shows the details of the FE model loading as well as boundary conditions.

2.2 Geometric Imperfections

In this study, FE simulation was consisted of two stages. In the first stage, an eigenvalue elastic buckling analysis that is available in the ANSYS program was carried out on a perfectly straight specimens of the column cross-sections HSS1 and HSS2. This stage aimed to establish the

probable buckling modes of the columns for different overall slenderness ratios (kL/r) of 10, 30, 46, and 58. The column behavior was also experimentally demonstrated for specimens with the same slenderness ratios. Sectional geometric imperfections can be considered in the FEA by assuming the elastic buckling modes obtained by the eigenvalue elastic buckling analysis is the imperfect shape of the columns. The buckling shape was first normalized so that the maximum displaced point was set equal to unity. Then, the desired value of imperfection was multiplied by this normalized shape. Because the sectional imperfections have no remarkable effect on the ultimate axial capacity of the columns, then the effect of the sectional imperfections was ignored, M. A. El Aghoury et al. [22]. The out-of-straightness geometrical imperfections have been modeled by assuming the column bent about the minor axis in a half sine wave in the direction that causes compression, with its apex at the column mid-height. The out-of-straightness values at mid-height of the columns, experimented by El-Sayed et al. [1], were provided in the FE modeling to initiate the overall buckling mode of failure, indicated by the eigenvalue elastic buckling analysis (first stage analysis).The measured out-of-straightness (e') in both sides of the column are listed in Table 2. The out-of-straightness ranged from L/4855 to L/847, and the highest value was L/1891. For overall geometric imperfections, L/1000 is usually used as the initial geometric imperfection value based on ANSI/AISC 303. Fig. 2 shows an example of overall geometric imperfections profile measured for specimen S80L46T6.

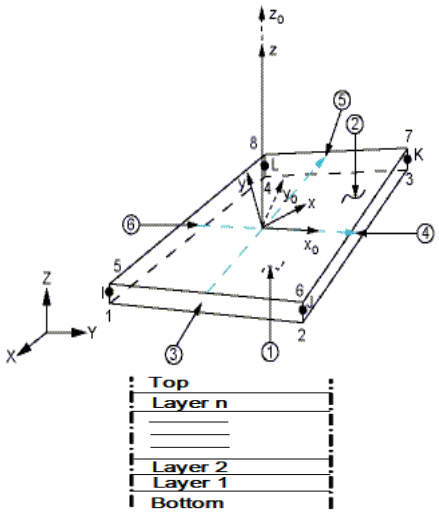

(a) Geometry of 4-node layered SHELL 181

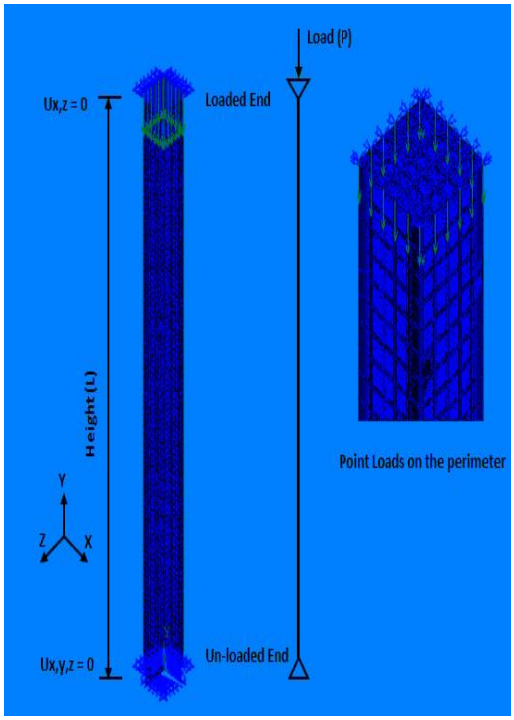

(b) FE Model loading and boundary conditions

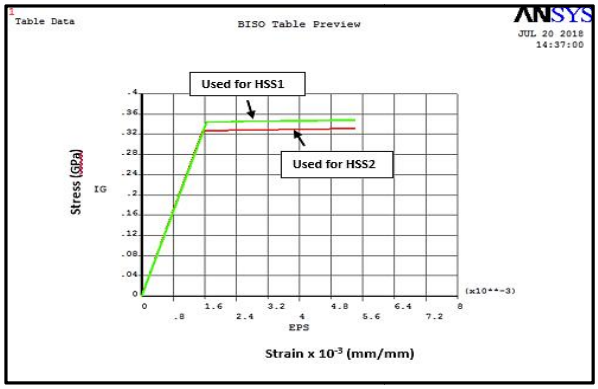

(c) Steel stress-strain curve used in the FEM

Fig. 1. Finite element modeling

2.3 Residual Stresses

In the proposed FE model, through-thickness residual stress distribution is idealized as shown in Fig. 3. Residual stresses, f_{rs} was obtained from the compression tests conducted on HSS stub-columns, El-Sayed et al. [1]. The residual stresses values were equal to $0.48f_y$ and $0.33f_y$ for HSS1 and HSS2 sections, respectively. In order to simulate through-thickness residual stresses pattern, a simplified approach was used, Shaat and Fam [13]. The residual stress pattern across the wall thickness was first defined by dividing the steel wall in the used multi-layer steel shell element (SHELL181) into three equal layers, as given in Fig. 3. The residual stress was defined by shifting origin of the axes of the stress-strain curve of the steel material of each layer along the linear part of the curve upwards or downwards, depending on whether the residual stress is compression or tension. The considered residual stress component with respect to the used shell element local coordinate system equals to the magnitude of the shift as follows: for inner layer a uniform compressive stress value of ($-f_{rs}$) was assigned, while a tensile stress value of ($+f_{rs}$) was assigned to the outer layer. The middle layer was also divided into two equal halves. A uniform value of ($-0.5f_{rs}$) was assigned to the inner half, while the outer half was assigned a uniform value of ($+0.5f_{rs}$). The membrane residual stresses was ignored in this FE analysis because it was considered insignificant, relative to the through-thickness residual stress.

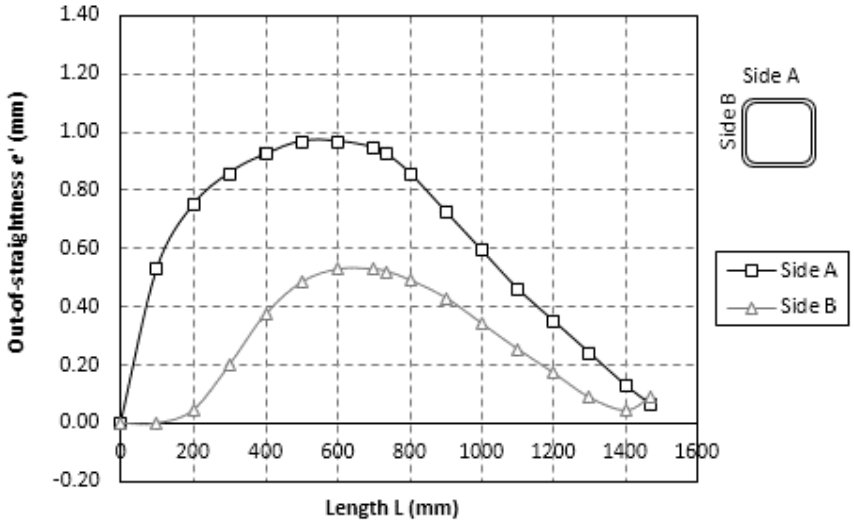

Fig. 2. Overall geometric imperfection profile for S80L46T6

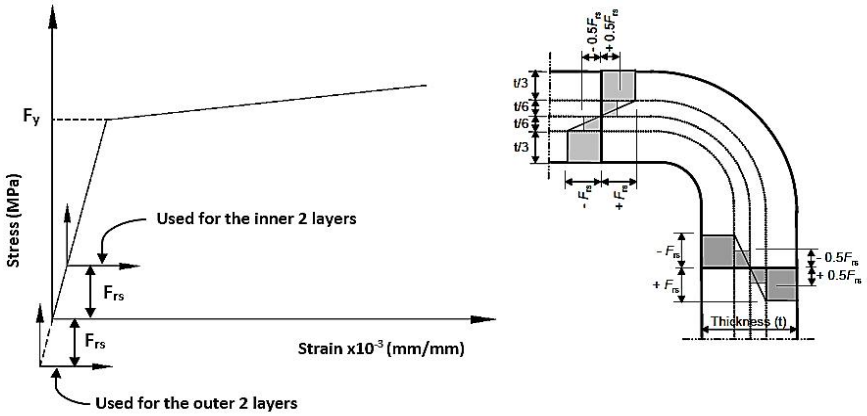

Fig. 3. Modeling of through-thickness residual stress

3. FE SIMULATION OF EXPERIMENTS

FE modeling introduces an alternative tool that is used in analysis and design, and also for verifying the obtained results with the previously done experiments, El-Sayed et al. [1]. Table 1 lists some basic data relevant to the experiments of El-Sayed et al. [1]. The failure modes were observed due to axial concentric loading applied on the tested column specimens. In control specimens, the failure mode shape predicted by the FE modeling, which is an overall buckling as in Fig. 4(a), is quite similar to the buckling failure mode observed in the experimented specimens as in Fig. 4(b). After excessive overall buckling occurred, the local buckling is observed in the slender long columns. While inward local buckling observed in the compression sides, outward local buckling observed in the other two sides for HSS specimens with a relatively large *b/t* ratio. Fig. 4(c) shows a typical local buckling observed approximately at mid-height of the experimented specimens. Figs. 4(d) and (e) show the same pattern of deformation predicted by the FE modeling, in terms of the nodal displacement contours in both x- and z-directions. The approximate similarity of deformations in Figs. 4(d), and (e) to 4(c) provides a confidence in the FE model. For mortar-strengthened specimens, crushing of mortar layer and steel yielding were only observed at the specimen ends as shown in Figs. 5(a) and (b).

Table 2 presents a comparison between the axial strength obtained from the numerical analysis and the experiments of El-Sayed et al. [1]. In general, very good agreement is shown between the FE models and the experimental test results for all columns with a maximum difference of 9%. The mean value of ($P_{FEM.}$ /$P_{EXP.}$) ratio is 1.022 and the standard deviation is 0.0539. The FE predicted versus experimented load-axial displacements (Δ) at the top end for all the column specimens are shown in Fig. 6. The figure shows a good convergence between the FE simulated and experimental results The axial displacement due to curvature from the (P-δ) effect depends on the chord length of the buckled column. This curvature observed experimentally was not perfectly symmetric, and may result in difference between the predicted and experimental results. The probable existence of eccentricity between the top loading point and the bottom reaction in the experiments can also attribute to this difference.

Table 1. Material Properties based on stub-column tests

Section	Modulus of Elasticity (GPa)	Prop. limit stress (MPa)	Yield strength (MPa)	Residual stress (F_{rs}/F_y)
HSS1	200	180	344	0.48
HSS2	200	218	327	0.33

Table 2. Comparison between experimental and numerical FE model results

Specimen		*kL/r*	Out of Straightness, *e'* (mm)		Axial strength, *P* (kN)		$P_{FEM.}$ / $P_{EXP.}$
Cross-section	ID		Side A	Side B	Experimental, $P_{EXP.}$ (kN)	FE model, $P_{FEM.}$ (kN)	
HSS1-	S80L30T0	30	0.92	0.41	91.53	98	1.07
80 x 80 x 1.5	S80L30T3	30	0.87	0.42	127.18	132	1.04
	S80L46T0	46	0.89	0.41	74.31	78	1.05
	S80L46T3	46	0.92	0.46	125.07	128	1.02
	S80L46T6	46	0.97	0.53	131.43	144	1.09
	S80L58T0	58	0.98	0.53	59.21	54	0.91
	S80L58T3	58	0.96	0.49	101.23	96	0.95
	S100L46T0	46	0.53	0.38	116.73	120	1.03
HSS2-	S100L46T3	46	0.54	0.40	166.74	170	1.02
100 x 100 x 1.5	S100L46T6	46	0.54	0.39	190.30	198	1.04
Mean							1.022
Standard deviation							0.054

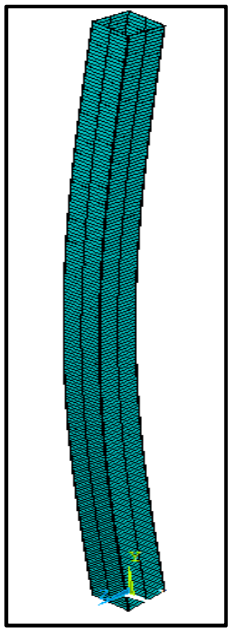

a) Overall buckling based on FE modeling

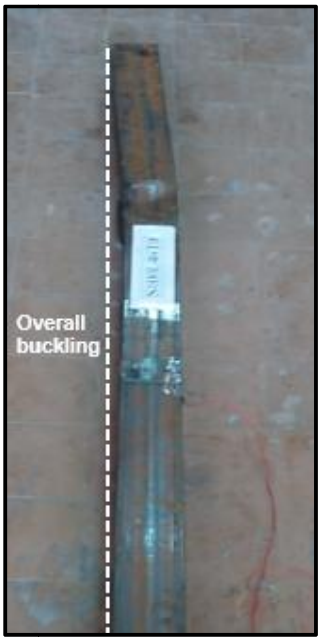

b) Overall buckling based on experiments

(c) Local buckling based on experiments

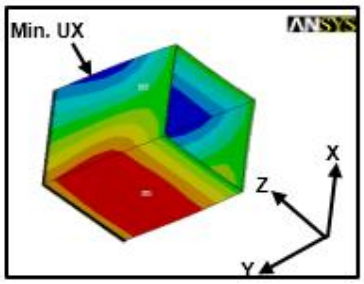

d) Nodal displacement in x-direction

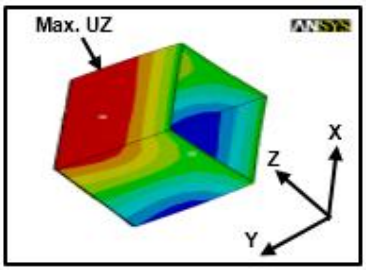

e) Nodal displacement in z-direction

Fig. 4. Comparison between the deformed shapes in experiments and FE Modeling for group A columns

The full responses of load versus lateral displacements (δ) for all column specimens, have been predicted and also compared with the experimental test result as given in Fig. 7. The FE models appear to somewhat overestimate the load versus lateral displacement relationship for some specimens especially at high slenderness ratio (kL/r = 58). Very good agreement is shown with the experimental test results for other column specimens. In these specimens, the global buckling observed in the experimental tests was in fact not symmetric. The maximum lateral displacement and failure occurred not perfectly at the middle. For this reason, the predicted load-lateral displacement relationship is different from the experimental one. In the post peak stage, some deviation between the experimented and FE analysis results are observed. The reason for such deviation may be due to the fact that an equivalent material has been used for polymer-mortar layers. When material non-linearity begins, different material undergoes incompatible strain followed by failure. The equivalency of such materials under highly complex non-linear state holds only approximately true. However, considering the load versus displacement overall responses, it can be said that a reasonably good agreement exists between experimental and FE analysis results. Thus the proposed FE model can be reliably used as a successful alternative for costly experimental tests.

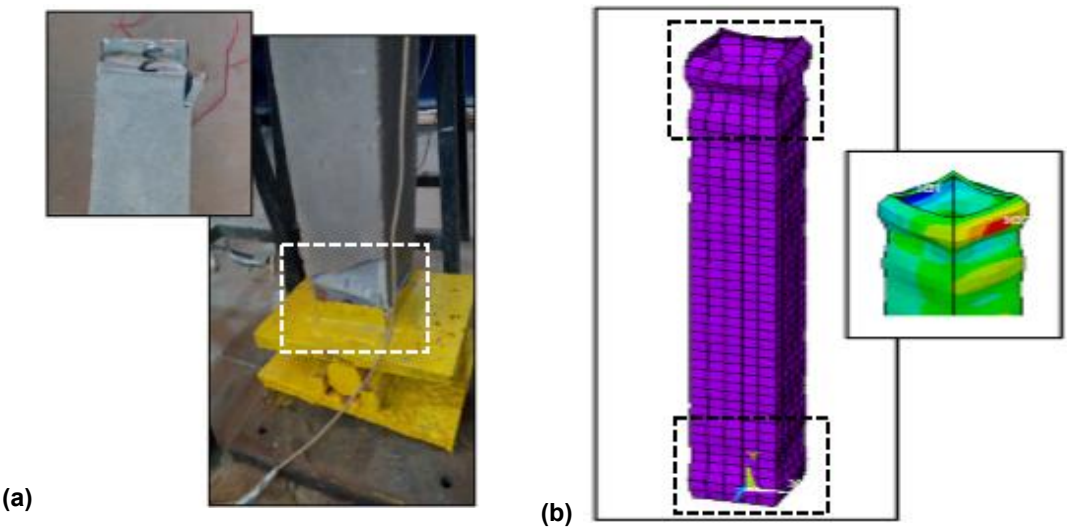

Fig. 5. Crushing of mortar and steel yielding at column ends

4. PARAMETRIC STUDY VARIABLES

To make an in-depth investigation for the axially loaded steel square HSS cold-formed columns strengthened with polymer-mortar, an extended parametric study was conducted using the proposed FE model. Preference has been given on the study of slender sections, since such sections are more susceptible to fail due to local buckling. A total of 76 selected slender AISC [19] square HSS column specimens with the same material properties as those used in the experimental analysis of El-Sayed et al. [1] were analyzed. The HSS columns chosen for the parametric study had different cross-sectional geometries or different flat width-to-thickness ratios $\lambda_b=b/t$, and different overall slenderness of columns $\lambda c=kl/r$. The flat width *(b)* considered were 75, 90, and 105 mm. Thickness of the steel square HSS section was kept constant equal to 1.5 mm. This means that the flat width-to-thickness ratios, λ_b, was equal to 50, 60, and 70. Members of different lengths were chosen to have a wide range of overall slenderness ratios ranging from 50 to 200. Thickness of the polymer-mortar strengthening layer (t_m equal to 0 (control), 2, 4, and 6 mm), was considered for conducting the parametric study, which was applied to the four sides of the square HSS column. Moreover, the value of initial out-of-straightness geometric imperfections at mid-height (e') ranged from L/500 to L/2000, where L is total length of the column. Sectional local geometric imperfection had no remarkable effect on the ultimate loads, therefore, this type of imperfection was ignored in the extended parametric study. Finally, the level of residual stress (F_{rs} = $0.25f_y$, and $0.5f_y$), where f_y is the steel yield strength as those used in the experimental analysis of El-Sayed et al. [1] was also studied. The following identification was used to identify the various cases of specimens in the parametric study. The first letter "S" represents the section profile (S = Square), while the following number reflects the flat width of the square HSS column (b). The following numbers specify the overall slenderness ratio of the column (λc), and the out-of-straightness geometric imperfection as a ratio of (L/e'). These numbers are followed by the residual stress level as a percentage of the yield stress (F_{rs} /F_y). Another number describing the polymer-mortar strengthening layer thickness (t_m) is also added at the end. For the unstrengthened control columns, the polymer-mortar strengthening layer thickness (t_m) equals zero. For example, "S75-50-500-25-4" describes a strengthened HSS column that has a flat width of 75mm, a member slenderness ratio of 50, a geometric imperfection of (Length/500), a residual stress level of 25% of its yield stress, and strengthened with 4 mm thickness of polymer-mortar strengthening layer. A summary of parametric study results is given in Table 3. Bar charts in Fig. 8(a) to (e) also show results obtained from the numerical simulation for all the HSS column specimens used in the parametric study with varying cross-sectional geometry, slenderness ratio, out-of-straightness, level of residual stresses, and polymer-mortar strengthening layer thickness.

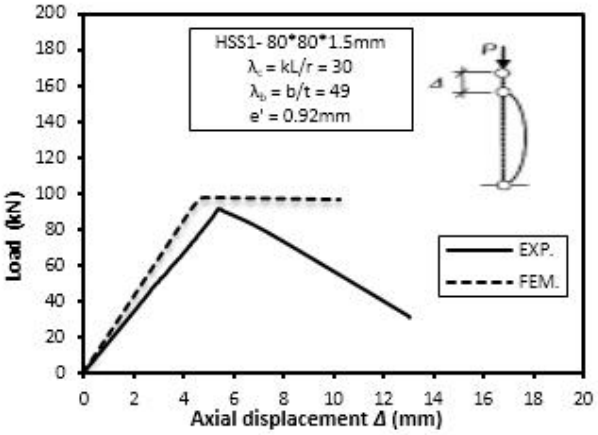

(a) **S80L30T0**

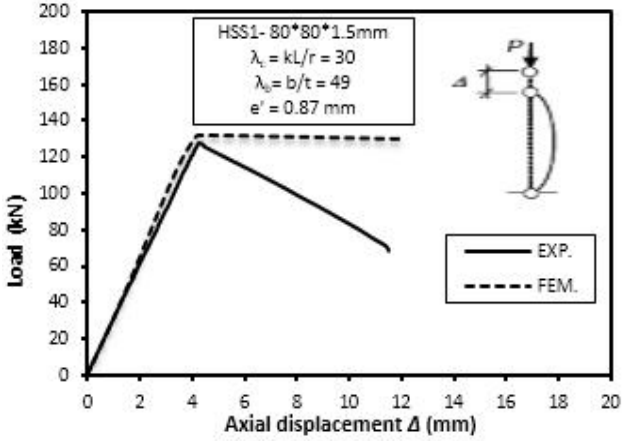

(b) **S80L30T3**

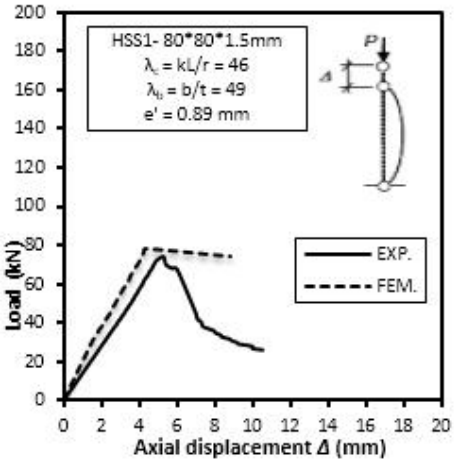

(c) **S80L46T0**

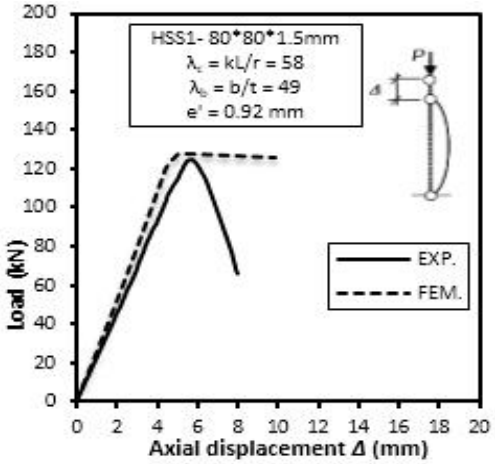

(d) **S80L46T3**

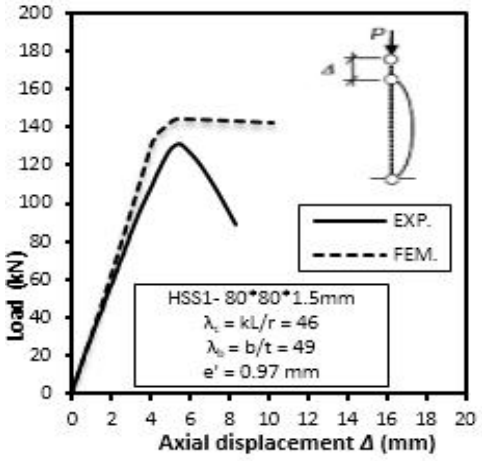

(e) **S80L46T6**

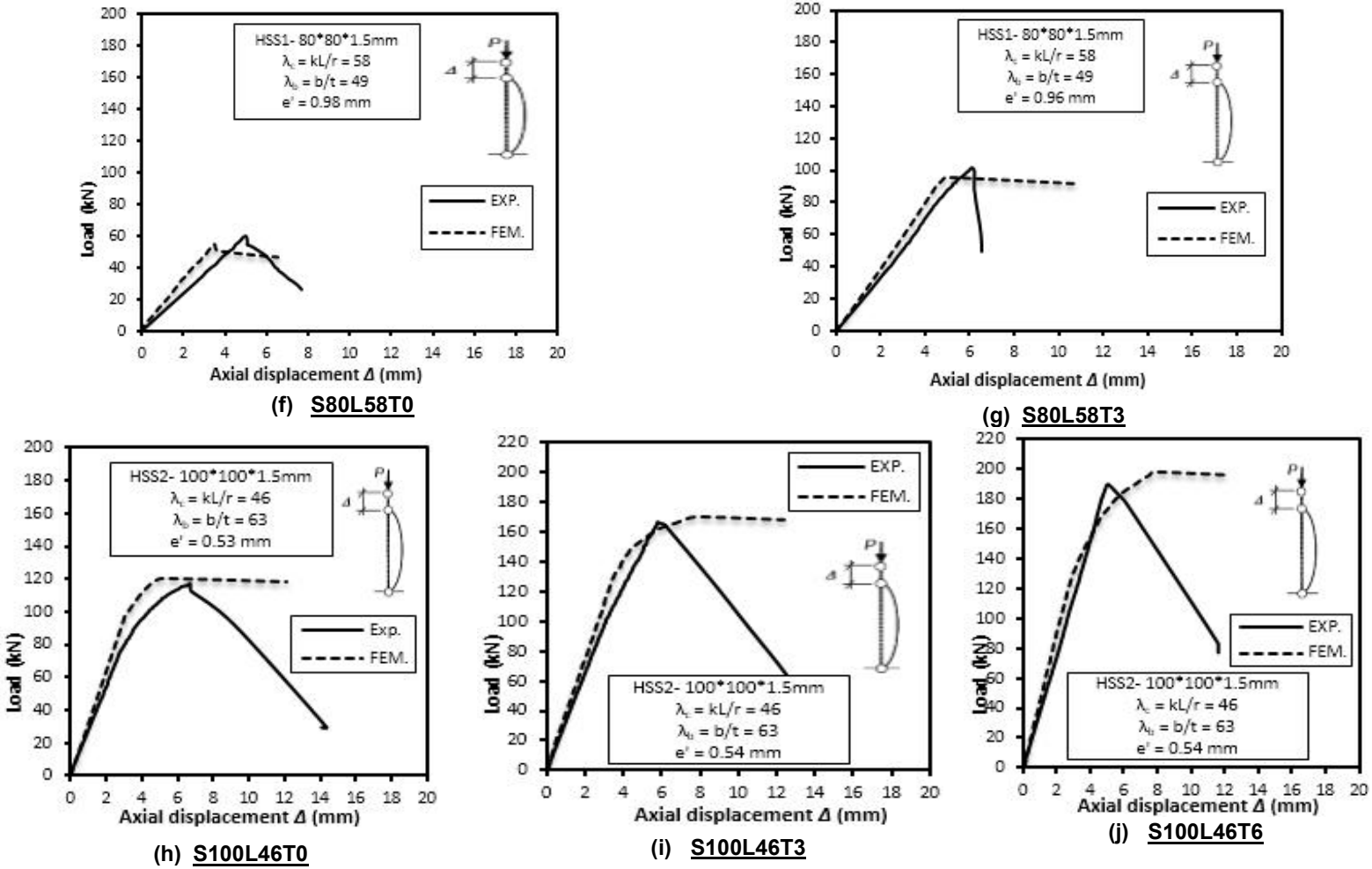

Fig. 6. Experimented and predicted load-axial displacement responses for unstrengthened/strengthened HSS column specimens

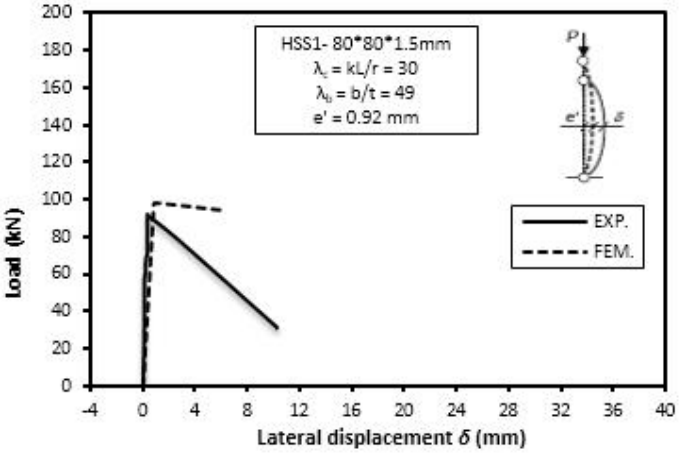

(a) **S80L30T0**

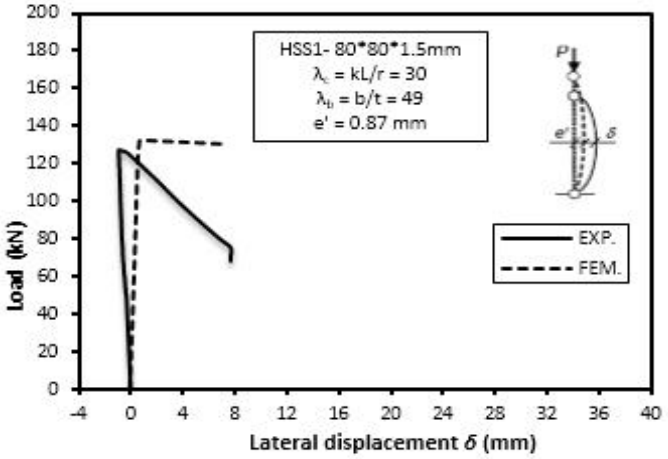

(b) **S80L30T3**

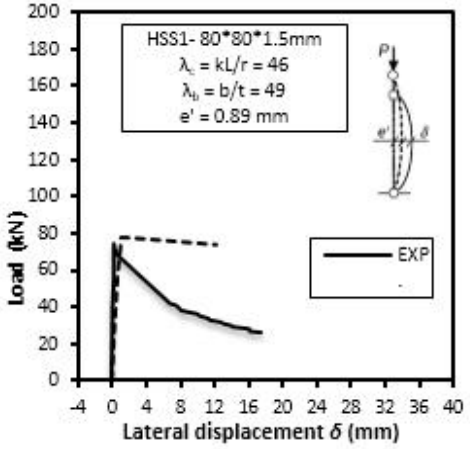

(c) **S80L46T0**

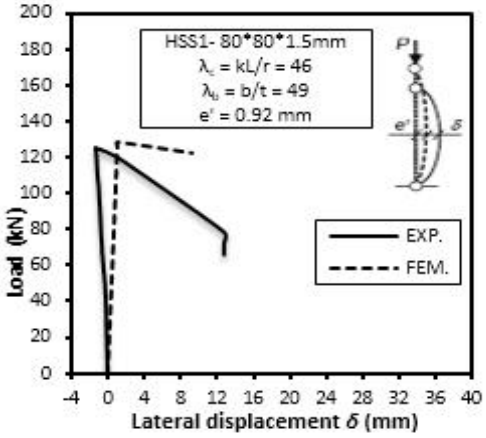

(d) **S80L46T3**

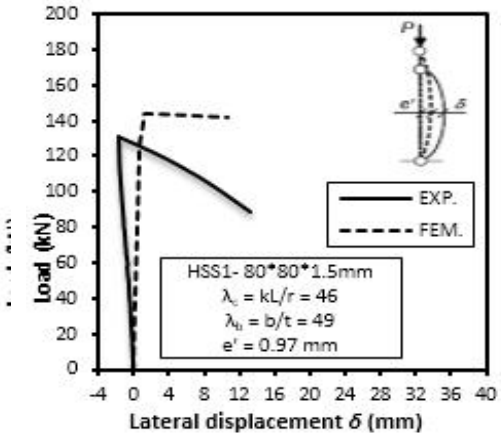

(e) **S80L46T6**

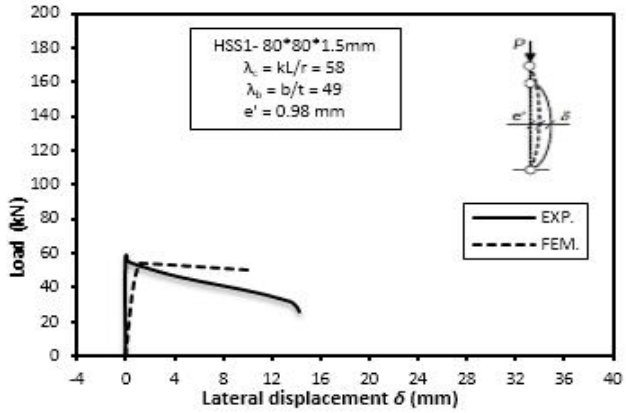

(f) **S80L58T0**

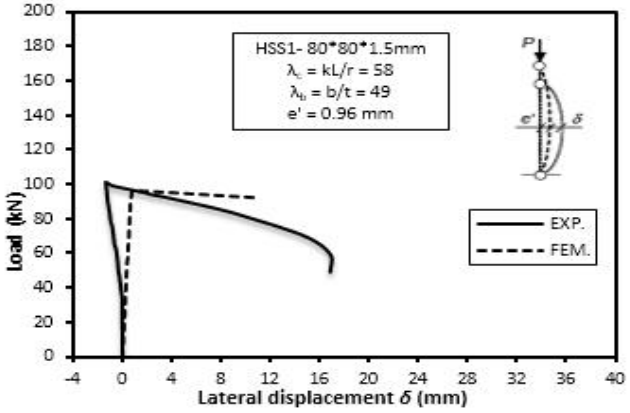

(g) **S80L58T3**

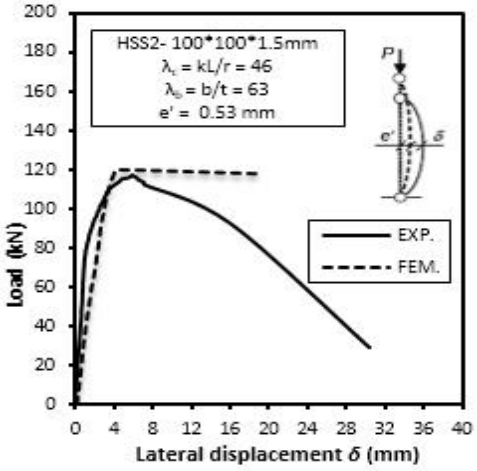

(h) **S100L46T0**

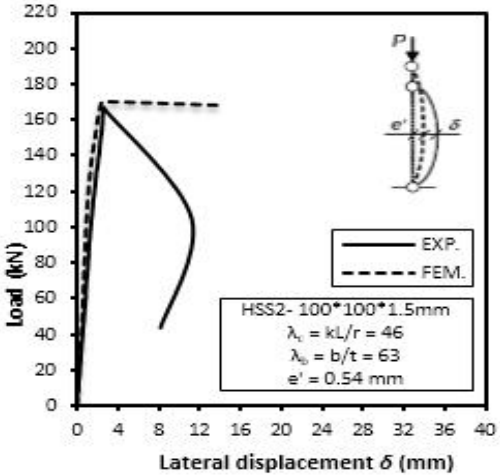

(i) **S100L46T3**

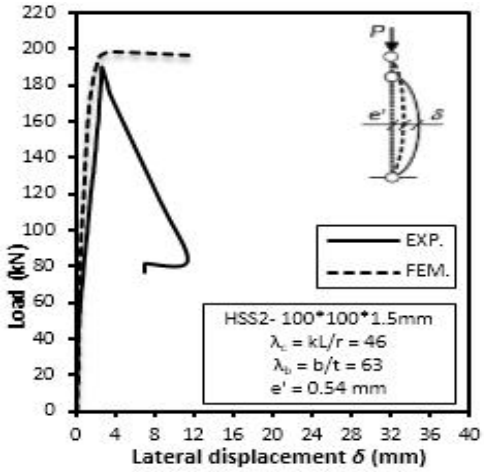

(j) **S100L46T6**

Fig. 7. Experimented and predicted load-lateral displacement responses for unstrengthened/strengthened HSS column specimens

5. RESULTS AND DISCUSSION

5.1 Effect of Polymer-Mortar Layer Thickness

The effect of the polymer-mortar strengthening layer thickness on the behavior of the square HSS column sections under concentric compressive loading has been shown in Fig. 9. The figure clearly shows that application of polymer-mortar to the unstrengthened steel square HSS columns can increase their strength by up to 95%. This axial strength gain increases with the increase of the mortar strengthening layer thickness. Whenever the square HSS column is subjected to axial compressive loading, the external bonding of the strengthening mortar layer provides a sufficient restraining effect against the elastic deformation which delays the local buckling, and as a result the ultimate axial strength is increased. Application of polymer-mortar causes an increase in the effective thickness ($t_{eff.}$) that reduces the width-to-thickness ratio of the cross-sectional elements. This decrease in the plate slenderness of the cross-sectional elements

Table 3. Summary of the parametric study results

Set	Models	Section parameters					P_u (kN)	% gain
		λ_b	λ_c	L/e'	F_{rs} / F_y	t_m (mm)		
1	S75-50-500-25-0	50	50	500	0.25	0	68	--
2	S75-50-500-25-2					2	96	41
3	S75-50-500-25-4					4	112	65
4	S75-50-500-25-6					6	120	76
5	S90-50-500-25-0	60				0	102	--
6	S90-50-500-25-2					2	136	33
7	S90-50-500-25-4					4	160	57
8	S90-50-500-25-6					6	168	65
9	S105-50-500-25-0	70				0	132	--
10	S105-50-500-25-2					2	170	29
11	S105-50-500-25-4					4	186	41
12	S105-50-500-25-6					6	201	52
13	S75-80-500-25-0	50	80	500	0.25	0	52	--
14	S75-80-500-25-2					2	76	46
15	S75-80-500-25-4					4	88	69
16	S75-80-500-25-6					6	94	81
17	S90-80-500-25-0	60				0	82	--
18	S90-80-500-25-2					2	112	37
19	S90-80-500-25-4					4	134	63
20	S90-80-500-25-6					6	142	73
21	S105-80-500-25-0	70				0	122	--
22	S105-80-500-25-2					2	160	31
23	S105-80-500-25-4					4	176	44
24	S105-80-500-25-6					6	190	56
25	S75-100-500-25-0	50	100	500	0.25	0	44	--
26	S75-100-500-25-2					2	66	50
27	S75-100-500-25-4					4	76	73
28	S75-100-500-25-6					6	82	86
29	S90-100-500-25-0	60				0	68	--
30	S90-100-500-25-2					2	98	44
31	S90-100-500-25-4					4	116	71
32	S90-100-500-25-6					6	122	79
33	S105-100-500-25-0	70				0	108	--
34	S105-100-500-25-2					2	146	35
35	S105-100-500-25-4					4	160	48
36	S105-100-500-25-6					6	180	67

(Continued on next page)

** Note. - Plate slenderness λ_b = b/t = 50, 60, and 70.*
- Overall slenderness λ_c = kL/r = 50, 80, 100, 150, and 200.
- Out-of-straightness L/e'=500, 750, 1000, and 2000. - Residual stresses F_{rs}/F_y = 25% and 50%.

Table 3. ***(Continued)***

Set	Models	Section parameters					P_u (kN)	% gain
		λ_b	λ_c	L/e'	F_{rs} / F_y	t_m (mm)		
37	S75-150-500-25-0	50	150	500	0.25	0	32	--
38	S75-150-500-25-2					2	52	63
39	S75-150-500-25-4					4	58	81
40	S75-150-500-25-6					6	62	94
41	S90-150-500-25-0	60				0	48	--
42	S90-150-500-25-2					2	76	58
43	S90-150-500-25-4					4	86	79
44	S90-150-500-25-6					6	90	88
45	S105-150-500-25-0	70				0	80	--
46	S105-150-500-25-2					2	120	50
47	S105-150-500-25-4					4	130	63
48	S105-150-500-25-6					6	142	78
49	S75-200-500-25-0	50	200	500	0.25	0	22	--
50	S75-200-500-25-2					2	38	73
51	S75-200-500-25-4					4	41	86
52	S75-200-500-25-6					6	43	95
53	S90-200-500-25-0	60				0	38	--
54	S90-200-500-25-2					2	64	68
55	S90-200-500-25-4					4	70	84
56	S90-200-500-25-6					6	73	92
57	S105-200-500-25-0	70				0	48	--
58	S105-200-500-25-2					2	78	63
59	S105-200-500-25-4					4	86	79
60	S105-200-500-25-6					6	90	88
61	S75-50-750-25-0	50	50	750	0.25	0	76	--
62	S75-50-750-25-2					2	103	36
63	S75-50-750-25-4					4	114	50
64	S75-50-750-25-6					6	118	55
65	S75-50-1000-25-0	50	50	1000	0.25	0	82	--
66	S75-50-1000-25-2					2	105	28
67	S75-50-1000-25-4					4	116	41
68	S75-50-1000-25-6					6	120	46
69	S75-50-2000-25-0	50	50	2000	0.25	0	96	--
70	S75-50-2000-25-2					2	116	21
71	S75-50-2000-25-4					4	128	33
72	S75-50-2000-25-6					6	132	38
73	S75-50-500-50-0	50	50	500	0.50	0	66	--
74	S75-50-500-50-0					2	92	39
75	S75-50-500-50-0					4	105	59
76	S75-50-500-50-0					6	112	70

actually leads to a delayed local buckling which ultimately enhances the overall buckling strength of columns. An effective moment of inertia ($I_{eff.}$) is also changed due to the application of polymer-mortar. However, the effective moment of inertia varies from a section to another along the column yielded length and also varies with the applied load. The length of the yielded part of the column depends on many factors, including the overall slenderness ratio geometric imperfections profile, and level of residual stresses. As observed in Fig. 9(a) to (e), the increase percentage in axial strength decreases for higher slender sections (i.e. as the cross-section's geometry increases). These sections are more prone to failure where secondary local buckling may occur after overall buckling. Also shown in Fig. 9(f), the percentage increases in axial strength of strengthened specimens with mortar layer thickness t_m of 2, 4, and 6mm are 41, 65, and 76% for specimens with e'=L/500 and are 21, 33, and 38%, for specimens with e'=L/2000, respectively.

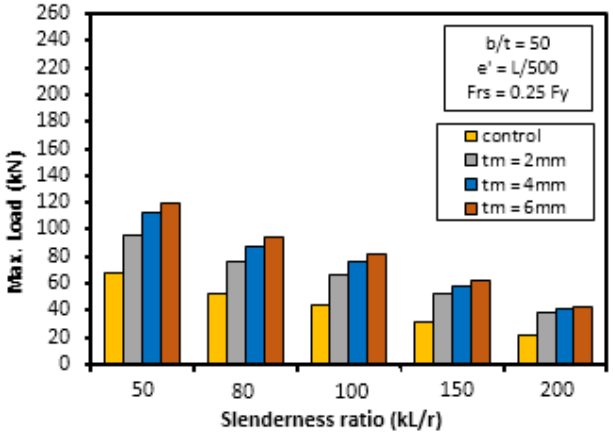

(a) **b/t = 50**

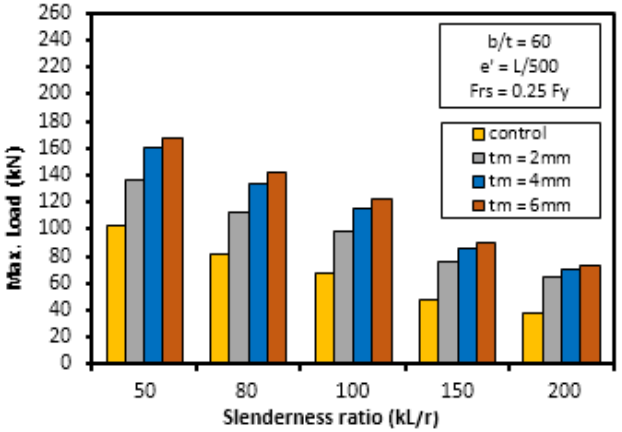

(b) **b/t = 60**

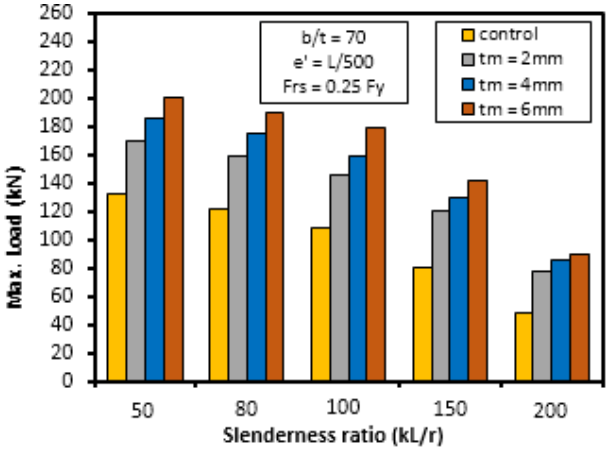

(c) **b/t = 70**

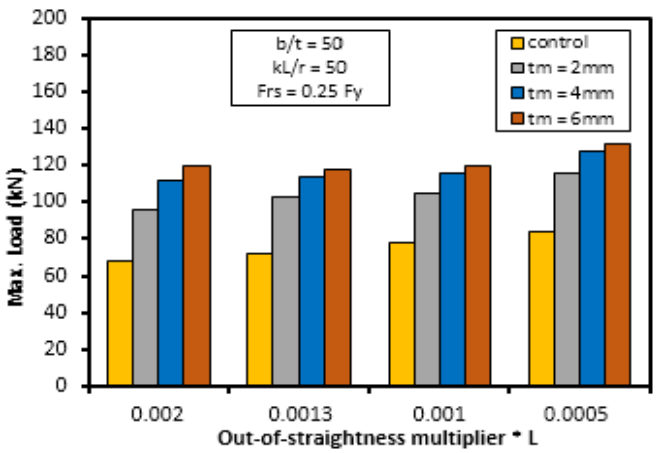

(d) Varying out-of-straightness.

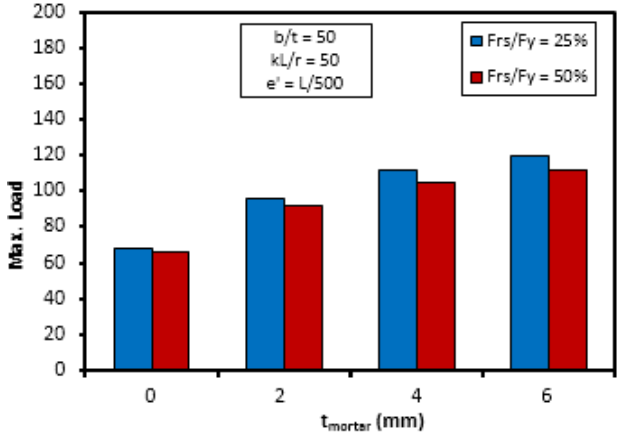

(e) Varying level of residual stress.

Fig. 8. Summary of parametric study results

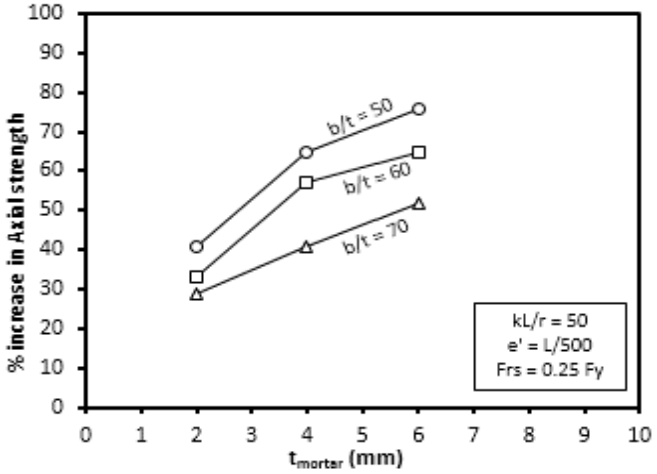

(a) **kL/r = 50**

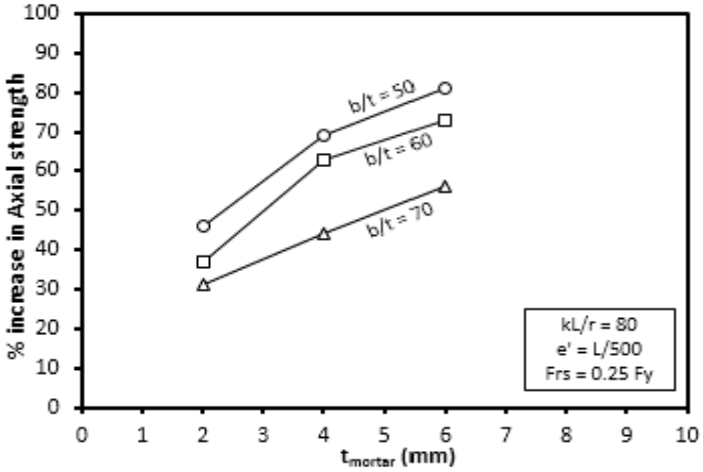

(b) **kL/r = 80**

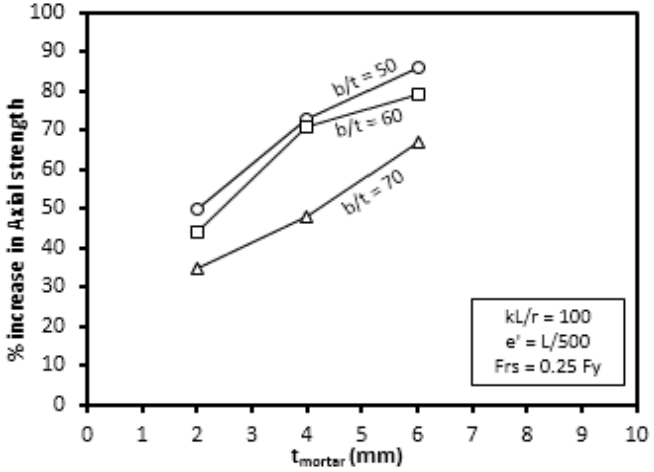

(c) **kL/r = 100**

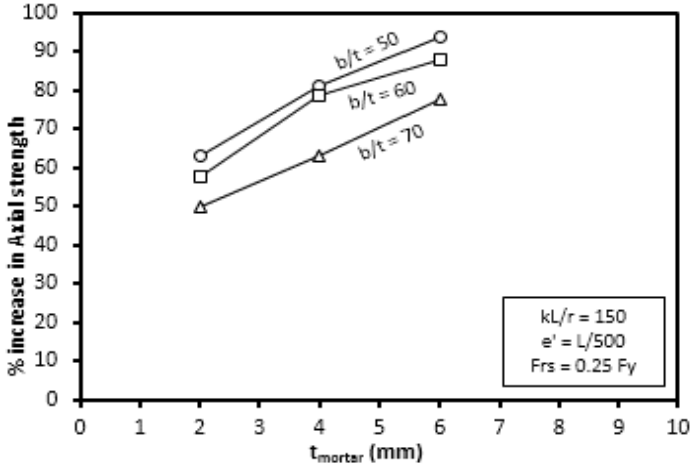

(d) **kL/r = 150**

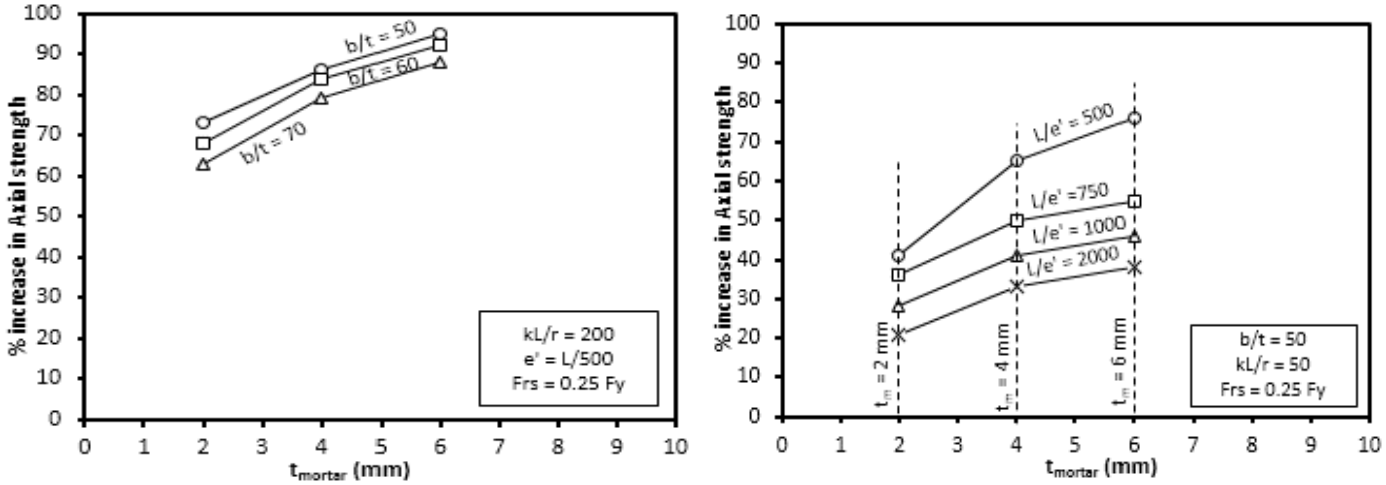

(e) kL/r = 200 **(f) Varying out-of-straightness.**

Fig. 9. Effect of polymer-mortar layer thickness on strength

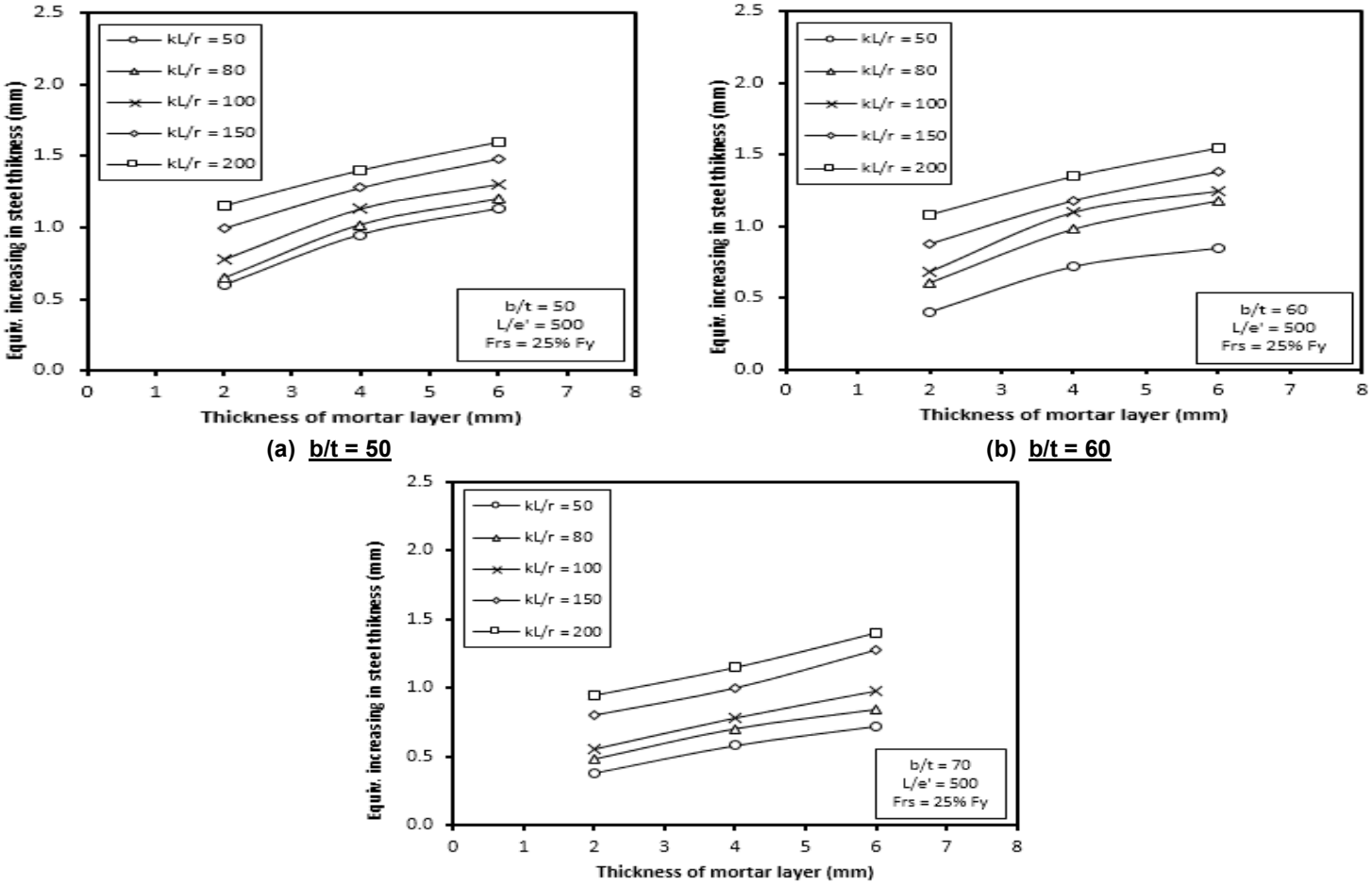

(a) b/t = 50

(b) b/t = 60

(c) b/t = 70

Fig. 10. Equivalent steel thickness

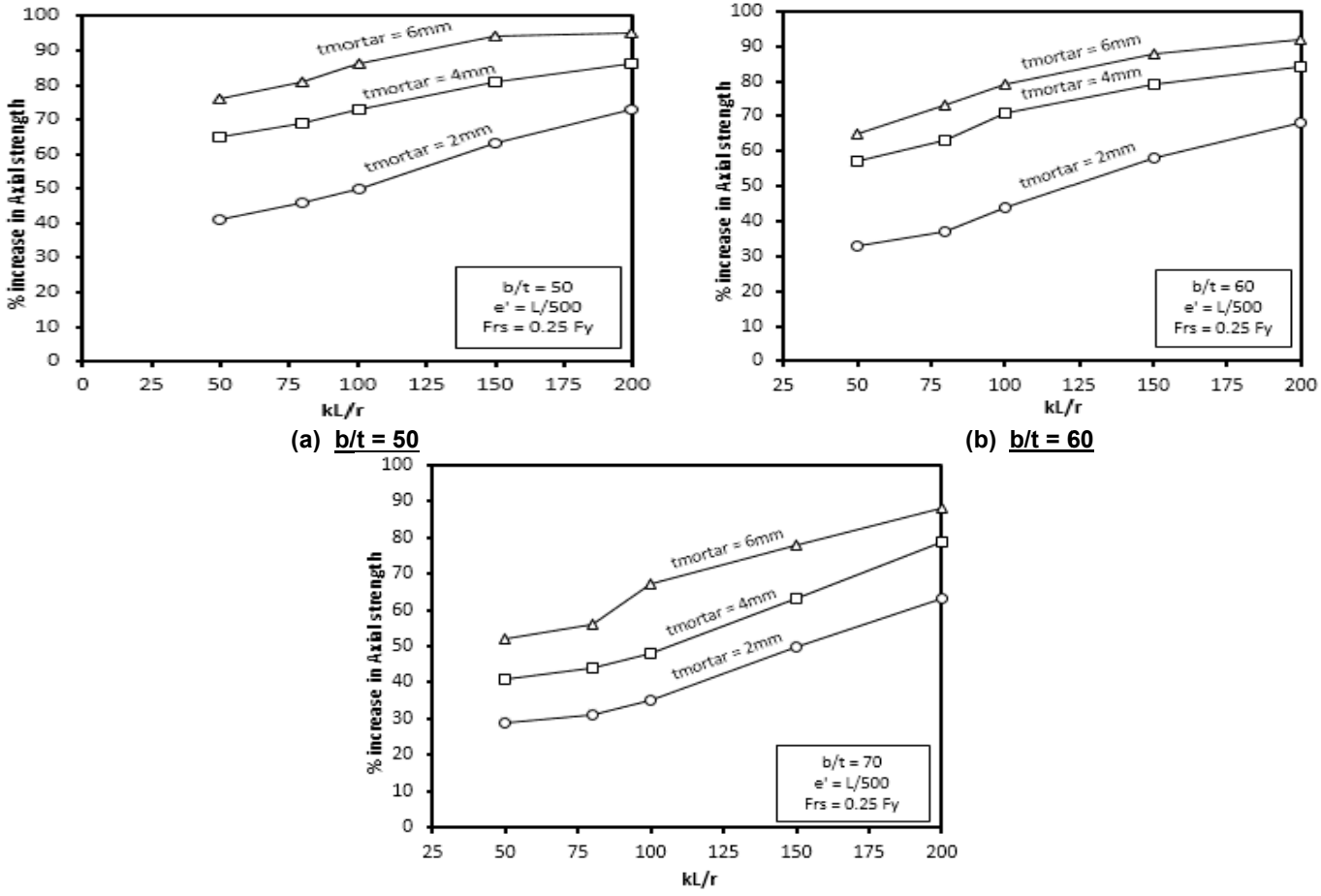

Fig. 11. Increase percentage in axial strength for different cross-sectional geometry

5.2 Equivalent Steel Thickness

In this section, an equivalent increasing in steel thickness is accounted for 45 polymer-mortar strengthened square HSS columns analyzed in the parametric study. It was concluded that application of mortar strengthening layer to the steel square HSS columns led to increase the steel thickness of the tube. Changing the polymer-mortar thickness from 2mm to 6mm were equivalent to increasing the steel tube thickness by as much as 40 to 107 % for specimens with b/t of 50, and by 27 to 103% for specimens with b/t of 60, as observed in Fig. 10. The steel tube thickness for highly slender specimens with b/t of 70 increased by up to 93%. It was also concluded that the increase percentage of equivalent steel thickness increases as overall slenderness ratio increases.

5.3 Effect of Cross-Sectional Geometry

In general, highly slender sections are more prone to the failure due to local buckling. For the relatively large square HSS columns, such as those with b/t ratio of 70, the increase percentage in axial strength is by about 29 to 88% due to polymer-mortar strengthening with increasing layer thickness of 2, 4, and 6mm as observed in Fig. 11(c). For higher slender section, addition of polymer-mortar layers may not significantly contribute in reducing the width-to-thickness ratio of the elements comprising these sections. Axial load capacity is generally governed by the local buckling which depends on b/t ratio of the cross-section. Since b/t ratio does not decrease significantly, the strength gain is also not significant. On the other hand, for small and medium steel square HSS sections, (i.e. with b/t of 50 and 60), the addition of mortar layers can significantly decrease the b/t ratio of the cross-section. This prevents or delays the onset of local buckling, resulting in increasing the axial strength up to 95% as given in Fig. 11(a), and (b).

5.4 Effect of Out-of-Straightness

The polymer-mortar strengthening layer thickness and the value of initial out-of-straightness have a combined effect on the column strength. Fig. 12 shows the variation of percentage increase of axial strength with the out-of-straightness values, for various polymer-mortar layer thicknesses. The polymer-mortar strengthening system is more effective for HSS columns with higher levels of out-of-straightness, particularly for specimens strengthened with mortar thickness of 4, and 6 mm, as given in Fig. 12. In general, the increase percentage in axial strength is reduced as the out-of-straightness decreases. However, for specimens strengthened with 2 mm at higher levels of out-of- straightness, the increase percentage in axial

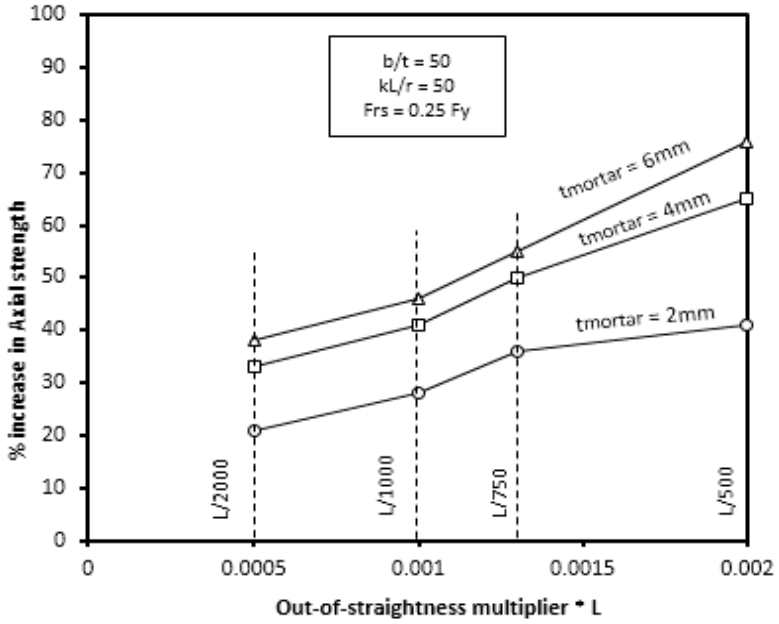

Fig. 12. Effect of out-of-straightness on strength

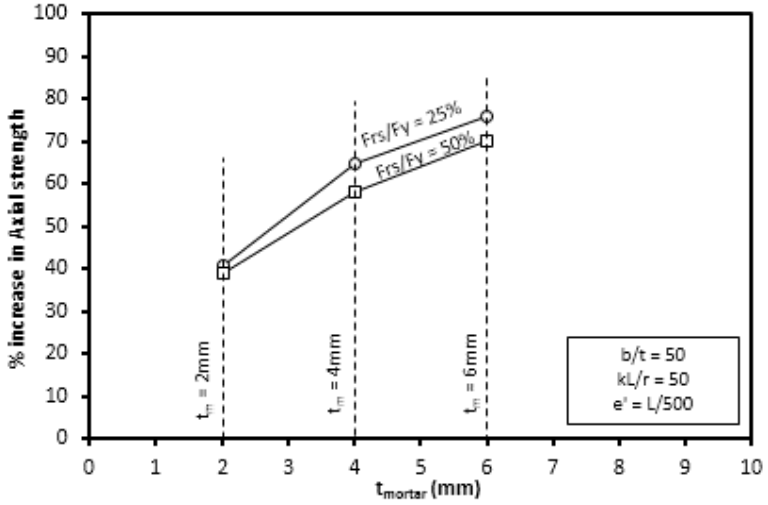

Fig. 13. Effect of residual stress on strength

strength seems to be independent of the level of out-of-straightness. At lower levels of out-of-straightness, both sides of the column specimen are under compression, while at higher levels, the polymer-mortar layer may be crushed only on the inner side. Although overall geometric imperfections affect the column strength before and after strengthening, the gain in strength is highly dependent on the mortar strengthening layer thickness and member slenderness ratio, rather than the value of imperfections.

5.5 Effect of Residual Stress

In this section, it was concluded that through-thickness residual stress has a slight effect on the increase of axial strength of HSS columns strengthened with polymer-mortar, as observed in Fig. 8(e) and Fig. 13. The figures also show that the lower the residual stresses, the higher the increase in column's axial strength. Fig. 8(e) shows that if the value of residual stresses increased from 25 to 50% of the steel yield stress, the maximum load of the unstrengthened specimen reduces from 68 kN to 66 kN, which represents only a 2.9% reduction. This reduction in maximum load reaches 6.7% for the specimen strengthened with 6mm thickness of polymer-mortar layer.

6. CONCLUSION

Axially-loaded strength of HSS steel column strengthened with polymer-mortar was investigated numerically using a three dimensional non-linear finite element model. Verification of this FE model has been demonstrated with reference to the experiments of El-Sayed et al. [1], where good agreement was found. This validates the ability of performing further study using this numerical model rather than conducting a relatively expensive experimental study. Then, the proposed model was used for performing an extended parametric study on 76 steel square HSS columns with varying cross-sectional geometries as well as overall slenderness ratios, strengthened with different mortar layer thicknesses. The effect of initial overall geometric imperfections at mid-height of the column and the level of residual stress were also considered.

Based on results of the parametric study, the following conclusions were drawn:

- Polymer-mortar materials are capable of increasing axial strength of the steel HSS slender columns. The column's axial strength can be increased by up to approximately two times that of unstrengthened specimens depending on the mortar layer thickness and slenderness ratio.
- The application of polymer-mortar increases the effective thickness reducing the width-to-thickness ratio of the cross-sectional elements which ultimately results in a delayed local buckling, and as a result increasing the overall buckling strength of columns.

- Application of polymer-mortar with thickness ranged between 2mm and 6mm was equivalent to an increase in the steel tube thickness by 27% to 107% for different dimensions considered in the parametric study.
- Axial load capacity is generally governed by the local buckling which depends on the width-to-thickness ratio of the cross-sectional elements. For highly slender sections, the axial strength gain due to polymer- mortar was about 29 to 88% and proportional to the thickness of mortar layers (2, 4 and 6 mm). On the other hand, for small and medium steel square HSS sections, there is a significant increase in strength due to mortar strengthening up to 95% with 6 mm mortar layer thickness.
- Polymer-mortar strengthening system is more effective for HSS columns with higher levels of out-of-straightness, particularly for specimens strengthened with mortar thickness of 4, and 6 mm. The increasing in axial strength is reduced as the out-of-straightness decreases.
- The level of through-thickness residual stress has a slight effect on the increase in axial strength of HSS columns strengthened with polymer-mortar. The increasing in axial strength is reduced as the level of residual stresses decreases.

ETHICAL APPROVAL

As per international standard written approval of Ethics committee has been collected and preserved by the author(s).

ACKNOWLEDGEMENTS

Authors are thankful to management and Director of Benha Faculty of Engineering, Benha University, Egypt, for rendering the necessary support to carry out this research.

COMPETING INTERESTS

Authors have declared that no competing interests exist.

REFERENCES

1. El-Sayed KM, Ahmed S. Debaiky, Nader N. Khalil, Ibrahim M. El-Shenawy. Improving buckling resistance of hollow structural steel columns strengthened with polymer-mortar. Thin-Walled Structures. 2019;137:515-526.
2. Torabi H, Shariati M. Buckling analysis of steel semi-spherical shells with square cutout under axial compression. Strength of Materials. 2014;46(4):531-542.
3. Jaehong Lee, Huu Thanh Nguyen, Seung-Eock Kim. Buckling and post buckling of thin-walled composite columns with intermediate-stiffened open cross-section under axial compression. International Journal of Steel Structures. 2009;9(3):175-184.
4. Bambach MR. 6-Strengthening of thin-walled (hollow) steel sections using fibre-reinforced polymer (FRP) composites. Rehabilitation of Metallic Civil Infrastructure using Fiber Reinforced Polymer (FRP) Composites. 2014;140-168.
5. Law KH, Gardner L. Buckling of elliptical hollow section members under combined compression and uniaxial bending. Journal of Constructional Steel Research. 2013; 86:1-16.
6. Key PW, Hancock GJ. An experimental investigation of the column behavior of cold formed square hollow sections. Research Rep. No. R493, School of Civil and Mining Engineering, University of Sydney, Sydney, Australia; 1985.
7. Vieira L, Rodrigo Gonçalves, Dinar Camotim. On the local buckling of RHS members under axial force and biaxial bending. Thin-Walled Structures. 2018; 129:10-19.
8. Zhao XL, Zhang L. State-of-the-art review on FRP strengthened steel structures. Engineering Structures. 2007;29(8):1808-1823.
9. Haedir J, Xiao-Ling Zhao. Design of short CFRP-reinforced steel tubular columns. Journal of Constructional Steel Research. 2011;67(3):497-509.
10. Shaat A, Fam A. Axial loading tests on short and long hollow structural steel columns retrofitted using carbon fibre reinforced polymers. Canadian Journal of Civil Engineering. 2006;33(4):458-470.
11. Shaat A, Fam A. Fiber-element model for slender HSS columns retrofitted with bonded high modulus composites. Journal of Structural Engineering, ASCE. 2007a; 133(1):85-95.
12. Shaat A, Fam A. Finite element analysis of slender HSS columns strengthened with

high modulus composites. Steel and Composite Structures. 2007b;7(1):19-34.
13. Shaat A, Fam A. Slender steel columns strengthened using high-modulus CFRP plates for buckling control. Journal of Structural Engineering, ASCE. 2009;13(1): 2-12.
14. Urmi Devi, Khan Mahmud Amanat. Non-linear finite element investigation on the behavior of CFRP strengthened steel square HSS columns under compression. International Journal of Steel Structures. 2015;15(3):671-680.
15. Ritchie A, Fam A, MacDougall C. Strengthening long steel columns of s-sections against global buckling around weak axis using CFRP plates of various moduli. Journal of Composites for Construction, ASCE. 2015;19(4).
16. Liu X, Nanni A, Silva Pedro F. Rehabilitation of compression steel members using FRP pipes filled with non-expansive and expansive light-weight concrete. Advances in Structural Engineering. 2005;8(2):129–41.
17. El-Tawil S, Ekiz E. Inhibiting steel brace buckling using carbon fiber- reinforced polymers large-scale tests. Journal of Structural Engineering. 2009;135(5):530-538.
18. Feng P, Sawulet B, Zhang YH, Ye LP, Bai Y. Experimental study on buckling resistance of steel members strengthened using FRP. International Journal of Structural Stability and Dynamics. 2012; 12(1):153–78.
19. ANSI/AISC 360-16, Specification for Structural Steel Buildings, American Institute of Steel Construction, Chicago, USA; 2016.
20. ANSYS program revision 14. ANSYS Inc., Canonsburg, PA.
21. Bruneau M, Uang C, Whittaker A. Ductile design of steel structures, McGraw-Hill, New York; 1998.
22. Aghoury MAEl, Hanna MT, Amosh EA. Effect of initial imperfections on axial strength of cold-formed steel single lipped sigma section. EUROSTEEL, Naples, Italy; 2014.

Peer-review history:
The peer review history for this paper can be accessed here:
http://www.sdiarticle4.com/review-history/53521